

See discussions, stats, and author profiles for this publication at: <https://www.researchgate.net/publication/272181336>

# Evaluation of Force Field Performance for High-Throughput Screening of Gas Uptake in Metal-Organic Frameworks

ARTICLE *in* THE JOURNAL OF PHYSICAL CHEMISTRY C · FEBRUARY 2015

Impact Factor: 4.77 · DOI: 10.1021/jp511674w

---

CITATIONS

3

---

READS

56

5 AUTHORS, INCLUDING:



Song Li

Huazhong University of Science and Technology

29 PUBLICATIONS 339 CITATIONS

SEE PROFILE

# Evaluation of Force Field Performance for High-Throughput Screening of Gas Uptake in Metal–Organic Frameworks

Jesse G. McDaniel,<sup>†</sup> Song Li,<sup>‡</sup> Emmanouil Tylianakis,<sup>§</sup> Randall Q. Snurr,<sup>‡</sup> and J. R. Schmidt<sup>\*,†</sup>

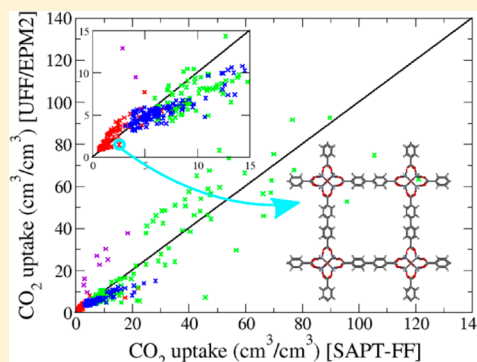
<sup>†</sup>Theoretical Chemistry Institute and Department of Chemistry, University of Wisconsin—Madison, 1101 University Avenue, Madison, Wisconsin 53706, United States

<sup>‡</sup>Department of Chemical and Biological Engineering, Northwestern University, 2145 Sheridan Road, Evanston, Illinois 60208, United States

<sup>§</sup>Department of Materials Science & Technology, University of Crete, Voutes Campus, Heraklion, Crete GR-71003, Greece

## S Supporting Information

**ABSTRACT:** High-throughput computational screening is an increasingly useful approach to identify promising nanoporous materials for gas separation and adsorption applications. The reliability of the screening hinges on the accuracy of the underlying force fields, which is often difficult to access systematically. To probe the accuracy of common force fields and to assess the sensitivity of the screening results to this accuracy, we have computed CO<sub>2</sub> and CH<sub>4</sub> gas adsorption isotherms in 424 metal–organic frameworks using *ab initio* force fields and evaluated the contribution of electrostatic, van der Waals, and polarization interactions on the predicted gas uptake and the adsorption site probability distributions. While there are significant quantitative differences between gas uptake predicted by standard (generic) force fields (such as UFF) and *ab initio* force fields, the force fields predict similar ranking of the MOFs, supporting the further use of generic force fields in high-throughput screening studies. However, we also find that isotherm predictions of standard force fields may benefit from significant error cancellation resulting from overestimation of dispersion and neglect of polarization; as such, caution is warranted, as this error cancellation may vary among different classes of materials.



## INTRODUCTION

Metal–organic frameworks (MOFs) have received a great deal of attention for applications including gas separation and storage, due primarily to their extremely high porosity and tunability. MOFs are synthesized through the self-assembly and crystallization of secondary-building units (SBUs), consisting of inorganic clusters acting as “nodes” connected by organic “linkers”, yielding millions of MOFs that could be potentially synthesized. Identifying and synthesizing promising candidate MOFs with tailored properties for specific application thus presents both a great opportunity and challenge.

High-throughput computational screening is becoming an increasingly popular tool to characterize large numbers of MOFs with respect to their gas adsorption and separation properties. Starting from ~30 000 experimentally documented metal–organic compounds in the Cambridge Structural Database, Watanabe and Sholl<sup>1</sup> identified 1163 structures as exhibiting a 3D network of connected atoms, and they computed CO<sub>2</sub> and N<sub>2</sub> gas adsorption and diffusion properties for a subset (359) that were deemed appropriately porous. Such efforts need not be restricted to materials that have been previously synthesized. Wilmer et al.<sup>2</sup> constructed a database of 137 953 hypothetical MOFs by exploiting the “building block” character of the constituent SBUs and screened these MOFs for their methane-storage capabilities. They identified hundreds of

candidate MOFs with higher methane storage than any existing material at the time. Other high-throughput screening studies of gas adsorption in MOFs have targeted hydrogen uptake and deliverable capacity,<sup>3</sup> CH<sub>4</sub>/H<sub>2</sub> separation,<sup>4</sup> and kinetically controlled gas separations.<sup>5</sup> In some cases, the resulting data have been further synthesized to develop quantitative structure–property relationships (QSPR) that correlate gas adsorption properties with structural characteristics of the materials, providing both valuable insight and a basis for efficient prescreening of candidate structures.<sup>6–10</sup> In addition, similar high-throughput screening studies have been conducted for gas adsorption/separation in zeolites.<sup>11–15</sup> For a comprehensive review of prior efforts regarding high-throughput screening of MOFs, we refer the interested reader to a recent review.<sup>16</sup>

All of these high-throughput screening applications rely on the ability to predict the gas-adsorption properties of MOFs with sufficient accuracy to yield meaningful results, while maintaining tractable computational efficiency. Grand canonical Monte Carlo (GCMC) simulations and variants, including hierarchically staged simulations,<sup>2</sup> graphics processing unit

Received: November 21, 2014

Revised: January 17, 2015

Published: January 21, 2015

(GPU) implementations,<sup>17</sup> and free energy grid-based lattice model simulations,<sup>18</sup> allow for efficient computation of gas adsorption isotherms. However, the ability to accurately predict the gas adsorption of a given MOF structure is limited by the force field utilized to describe the adsorbate–framework and adsorbate–adsorbate interactions. (This assumes an accurately known or hypothetically realistic MOF structure—the validity of this assumption is an important but separate question that is beyond the scope of the present work.) In light of ongoing work in this area, it is vital to critically evaluate the ability of commonly employed force fields to predict gas adsorption properties of MOFs and the robustness of high-throughput screening applications with respect to force field accuracy.

In this work, we compute gas adsorption isotherms for CO<sub>2</sub> and CH<sub>4</sub> for a diverse set of 424 MOFs, comparing the predicted uptakes from “standard” force fields commonly used in high-throughput MOF screenings to those predicted from accurate *ab initio* force fields. The latter are based on symmetry-adapted perturbation theory (SAPT)<sup>19</sup> and have been previously demonstrated to yield very accurate gas adsorption isotherms for a wide range of MOFs.<sup>20–23</sup> To our knowledge, this is the largest set of MOFs for which first-principles-derived force fields, including explicit adsorbate polarization, have been used to calculate gas adsorption isotherms. Our primary goal is to examine the robustness of high-throughput screening predictions to different treatments of electrostatic, van der Waals (vdW), and polarization interactions between adsorbates and MOF frameworks. This analysis provides important insights regarding the reliability of common “generic” Lennard-Jones force fields in high-throughput screening for gas adsorption. In addition, our study provides a quantitative analysis of the underlying physical mechanisms dictating gas adsorption for a large database of MOFs, revealing general principles that are important for future studies of gas adsorption in MOFs.

## METHODS

The hypothetical MOF structures were constructed based on previously reported methodologies.<sup>2</sup> The structures encompass three different topologies, pcu, fcu, and ftw, and are built from two different inorganic clusters, namely Zn<sub>4</sub>O and Zr<sub>6</sub>O<sub>4</sub>(OH)<sub>4</sub>, and 20 organic linkers. The organic linkers are shown in Figure S1 (Supporting Information); they are ditopic (e.g., the commonly employed benzenedicarboxylate (BDC) linker) and tetratopic linkers similar to those employed in ref 2 and in the recent MOF literature. The 10 ditopic linkers yield 10 pcu and 10 fcu structures, and the 10 tetratopic linkers yield 10 ftw structures. Most of the MOFs were generated by functionalizing the original 30 “parent” MOFs with seven functional groups. The linkers were either singly or doubly functionalized with one of the following groups: Cl, Br, NH<sub>2</sub>, NO<sub>2</sub>, OH, COH (aldehyde), or COOH. The functionalization was completed in an automated way using the in-house software FunctionalizeThis.<sup>24</sup> The obtained functionalized MOF structures were then optimized with constant cell size using the Forcite module in Materials Studio. To this set of 416 hypothetical MOFs, we added 8 experimentally known zeolitic imidazolate frameworks (ZIF-8, -25, -71, -68, -69, -78, -79, and -81) to increase structural diversity. It is important to note that none of the MOFs in this database contain coordinatively unsaturated metal sites, and thus there is no direct adsorbate–metal binding; modeling such systems may require specialized

force fields or techniques<sup>25,26</sup> and is beyond the scope of this work.

Isotherms for CO<sub>2</sub> and CH<sub>4</sub> were computed using our previously developed lattice-model based simulations.<sup>18</sup> Briefly, a free energy grid with  $\sim 1 \text{ \AA}^3$  resolution is constructed for each MOF by averaging the Boltzmann factor over thousands of randomly sampled configurations of the particular adsorbate within a grid cell. This free energy grid provides a quantitative topological picture of the adsorption sites and *exactly* determines the gas uptake in the low-pressure limit and maintains high accuracy through the saturation pressure. At higher pressure, we introduce “coarse-grained” adsorbate–adsorbate interaction potentials and run lattice-based GCMC simulations, yielding dramatic speed-ups over conventional fully atomistic GCMC simulations. We employed Ewald sums (PME<sup>27</sup>) to compute both electrostatic and vdW interactions out to infinite distance when generating the free energy grid. We note that only “pairwise” polarization effects are incorporated into the free energy grid, and true many-body polarization is not explicitly included; this should be a good approximation for computing CO<sub>2</sub> and CH<sub>4</sub> isotherms at low pressure. The resulting error in computed gas uptake of lattice-model simulations compared to fully atomistic GCMC simulations is negligible compared to the differences between force field predictions (see Figure S4 in Supporting Information). Simulation parameters of the lattice-model simulations are given in the Supporting Information.

The force fields that we employed can be classified into three types: (1) “standard” Lennard-Jones + Coulomb force fields describing adsorbate–MOF interactions; (2) SAPT-based, polarizable force fields describing adsorbate–MOF interactions; and (3) coarse-grained adsorbate–adsorbate potentials that are used in the lattice-model simulations. As prototypical examples of the “standard” force fields (and common choices in prior high-throughput screenings), we utilized the Lennard-Jones parameters from the universal force field (UFF)<sup>28</sup> for the MOF framework and the popular EPM2<sup>29</sup> (CO<sub>2</sub>) and TraPPE<sup>30</sup> (CH<sub>4</sub>) force fields for the adsorbate molecules. (Our general conclusions are not dependent on this specific choice; see Figures S4 and S5 in the Supporting Information.) The latter have been thoroughly benchmarked against neat fluid properties. The SAPT-based force fields (henceforth SAPT-FFs) have been previously described,<sup>21,22</sup> and we only briefly summarize here. These entirely *ab initio* force fields employ an explicit energy decomposition, with a one-to-one correspondence with the physically distinct intermolecular interaction energies of SAPT, namely electrostatics, exchange, induction, and dispersion. The exchange and other short-range interactions are treated with an exponential term, with damped  $C_n/R^n$  interaction terms ( $n = 6, 8, 10, 12$ ) for dispersion, accounting for higher-order interactions. McDaniel et al. previously found that a highly accurate treatment of dispersion interactions is necessary for quantitatively predicting CO<sub>2</sub> uptake in ZIFs.<sup>21</sup> Explicit polarization is treated using Drude oscillators (for CO<sub>2</sub><sup>31</sup>). All parameters of SAPT-FF used in this work are given in the Supporting Information. The lattice GCMC simulations also require coarse-grained adsorbate–adsorbate potentials. For CO<sub>2</sub> we employ the potential of Liu,<sup>32</sup> while for CH<sub>4</sub> we use the TraPPE force field.<sup>30</sup>

It is widely recognized that an accurate description of electrostatic interactions is vital for predicting gas uptake (aside from nonpolar methane and noble gases). Correspondingly, there has been significant work to model these interactions

using methods that are efficient enough for high-throughput screening.<sup>33–35</sup> In this work, we obtain *ab initio* charges for each MOF using an efficient fragment approach. Making use of the “building block” nature of MOFs, we deconstruct the MOF into its inorganic and organic SBUs. These individual SBUs are then terminated with capping atoms, and DFT calculations followed by subsequent distributed multipole analysis (DMA)<sup>36,37</sup> and charge fitting<sup>38</sup> to the DMA are carried out for each unique capped SBU (these charges are henceforth termed “ $Q_{\text{SBU}}$ ”). If the capping of these SBUs mimics the appropriate charge transfer between SBU units, then the derived atomic charges should be transferable to the bulk MOF, yielding an electrically neutral MOF. Validating this approach, we thus find only small net charge on each MOF (average absolute charge of 0.008  $e/\text{atom}$ , with the maximally charged MOF exhibiting an absolute charge of 0.016  $e/\text{atom}$ ). We evenly “smear” a neutralizing charge among the constituent atoms to generate a neutral system. This charge fitting procedure is described in detail in the Supporting Information.

## RESULTS AND DISCUSSION

All  $\text{CO}_2$  uptakes reported in this paper have been computed at 298 K and 0.2 bar (representative of the partial pressure under flue gas conditions) and are given in absolute uptake (volume of gas at STP adsorbed per volume of MOF). Calculations at 1 bar are given in the Supporting Information (Figures S8–S12), with almost identical conclusions.

We use two different metrics to quantify the degree of correlation between predicted uptakes. In a high-throughput screening application, there may be a hierarchy of methods applied to analyze a database of MOFs. For example, a computationally inexpensive method with lower accuracy might be used as an initial prescreening, followed by a higher accuracy, more expensive method applied to a subset of the top performing materials as predicted by the inexpensive method. In the initial screening, it is therefore highly important to correctly *rank* the MOFs in order of performance, so that the subset of highest performing materials is correctly identified for further screening. We therefore calculate the Spearman rank correlation coefficient (SRCC) as a measure of the ability of a particular method to successfully rank the MOFs by performance (we report the square of this value,  $\text{SRCC}^2$ , for consistency with the reported Pearson correlation). The higher accuracy method, on the other hand, should make accurate *quantitative* predictions of the gas uptake of the MOFs, so that the top performing candidates can be compared with previously characterized, existing materials. We therefore perform a linear regression (constraining the intercept to zero) on the uptake data predicted by one method versus that predicted by another method. We report both the slope and  $R^2$  values (square of the Pearson correlation coefficient) of this regression. All quantitative metrics are given in the corresponding figure captions. We note that all “lines” depicted in the figures in this paper correspond to the  $y = x$  line and serve to guide the eye; these lines do not represent the best-fit lines of the linear regression, and only the slope and  $R^2$  values of the regression are given.

**Comparison of Electrostatic Treatments for Predicting  $\text{CO}_2$  adsorption in MOFs.** Accurate treatment of electrostatic interactions between adsorbates and MOFs is crucial for predicting  $\text{CO}_2$  uptake. Here we compare  $\text{CO}_2$  adsorption predicted by three different charge derivation schemes, in combination with the UFF/EPM2 force field.

Note that even though the same force field is used to model vdW interactions in each case, the qualitative conclusions are somewhat dependent on the choice of force field because force fields determine the *ratio* of vdW to electrostatic interaction energies within the MOF. This ratio then determines the sensitivity of the computed uptake to the different charge-fitting schemes (see Supporting Information).

We first compare our  $Q_{\text{SBU}}$  charge fitting method to the REPEAT charge fitting method of Campana and co-workers<sup>39</sup> (see also Chen et al.<sup>40</sup>). In REPEAT, charges are fit to the electrostatic potential (ESP) generated by plane-wave DFT calculated electron densities in periodic systems. While this method has previously been used as an accurate “benchmark” to compare with other charge fitting schemes for MOFs,<sup>35,39,41</sup> it is probably too computationally expensive to be utilized in many high-throughput screening applications, especially for MOFs with large unit cells. In Figure 1, we compare the  $\text{CO}_2$

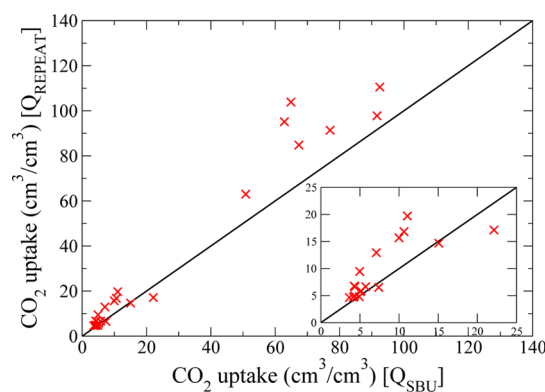


**Figure 1.**  $\text{CO}_2$  uptake for 24 MOFs computed using REPEAT charges ( $Q_{\text{REPEAT}}$ ) compared to that using  $Q_{\text{SBU}}$  charges (red symbols; black line is  $y = x$  to guide the eye).  $\text{SRCC}^2 = 0.86$ ,  $R^2 = 0.96$ , and slope = 1.25.

uptake for 24 MOFs as computed using REPEAT derived charges compared to  $Q_{\text{SBU}}$  charges. While the 24 MOFs were chosen for computational convenience based on their relatively small unit cells (less than  $\sim 20 \text{ \AA}^3$ ), they encompass all functional groups studied, and their  $\text{CO}_2$  uptakes span the range present in the full set of 424 MOFs.

There is satisfactory agreement between uptakes predicted by the two different charge fitting methods. While there do exist quantitative differences (slope = 1.25), there is good correlation ( $\text{SRCC}^2 = 0.86$ ,  $R^2 = 0.96$ ) between the predictions from the two charge methods. Neither method should be considered a “benchmark”, as both methods have potential limitations: the  $Q_{\text{SBU}}$  charges are generated from cluster models, while the REPEAT method can lead to unphysical charges on buried atoms.<sup>41</sup> However, the semiquantitative agreement between these methods gives confidence that the  $Q_{\text{SBU}}$  charge fitting scheme is robust and accurate enough for the purposes of this work. We note that we have employed this  $Q_{\text{SBU}}$  charge fitting scheme in previous works that have reproduced experimental adsorption isotherms in MOFs with excellent results.<sup>20,21,23</sup>

Methods for deriving charges for MOFs based on the charge equilibration (QEq) method of Rappe and Goddard<sup>42</sup> are a common choice in high-throughput screening due to their general applicability and computational efficiency.<sup>33–35</sup> Here we examine the MOF electrostatic-potential-optimized charge scheme (MEPO-QEq) of Kadantsev et al.,<sup>35</sup> in which the QEq



method is extended to periodic systems<sup>34</sup> and specifically reparameterized for 543 MOFs based on fitting to *ab initio* computed ESPs. All MEPO-QEq parameters were taken from the work of Kadantsev et al., except for Zr where the original QEq parameters were used (Zr was not refit in ref 35). We used an analogous periodic-QEq algorithm to that described previously by Haldoupis et al.<sup>34</sup> Figure 2 compares the

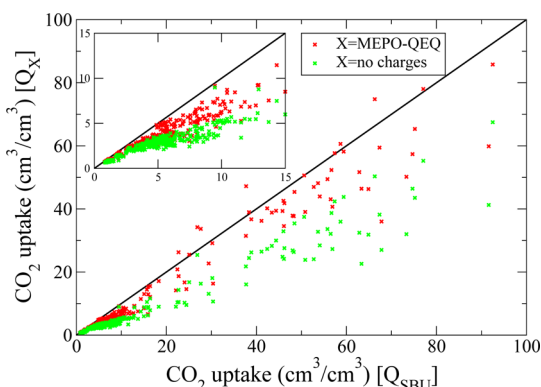


**Figure 2.** CO<sub>2</sub> uptake computed using MEPO-QEq charges compared to that using  $Q_{\text{SBU}}$  charges (red symbols):  $\text{SRCC}^2 = 0.94$ ,  $R^2 = 0.96$ , slope = 0.84. CO<sub>2</sub> uptake computed using no charges compared to that using  $Q_{\text{SBU}}$  charges (green symbols):  $\text{SRCC}^2 = 0.90$ ,  $R^2 = 0.94$ , slope = 0.58. The black line is  $y = x$  to guide the eye.

predicted CO<sub>2</sub> uptake using MEPO-QEq charges, no charges, and our  $Q_{\text{SBU}}$  charges. The correlation coefficients as well as the slope(s) of the best fit line(s) are very similar to those reported in ref 35 (note we report the *squares* of the correlation coefficients), although we have used a different “benchmark” charge method ( $Q_{\text{SBU}}$ ). The uptakes predicted by the MEPO-QEq method are modestly but systematically underestimated. While the correlation coefficients are high for predicted uptakes using the MEPO-QEq method compared to our  $Q_{\text{SBU}}$  method ( $\text{SRCC}^2 = 0.94$ ,  $R^2 = 0.96$ ), they are (quite surprisingly) also high for the analogous comparison *without any* charges ( $\text{SRCC}^2 = 0.90$ ,  $R^2 = 0.94$ ). Note that the contribution of electrostatics is overall very significant, as computed uptakes are dramatically lower when computed without charges. Differences between these electrostatic treatments are further magnified if explicit polarization of gas molecules is taken into account (*vide infra*). An analogous comparison between predicted CO<sub>2</sub> uptake for the same electrostatic treatments with the SAPT-FF force field for vdW interactions is given in the Supporting Information (Figures S6 and S7). Interestingly, in that case there is qualitatively worse agreement between gas-uptake predictions using MEPO-QEq charges and no charges as compared to  $Q_{\text{SBU}}$  charges. The differences in the conclusions are due to systematic differences in the strength of vdW interactions between UFF and SAPT-FF.

All subsequent calculations employ our  $Q_{\text{SBU}}$  charges for MOFs so as to isolate the importance of vdW and polarization interactions while using a consistent and accurate treatment of electrostatics.

#### Analysis of vdW and Polarization Force Field Components for Predicting CO<sub>2</sub> Adsorption in MOFs.

In conjunction with electrostatics, the force field chosen to describe adsorbate–MOF vdW interactions governs the predicted gas uptake. To the best of our knowledge, all previous high-throughput screening studies of gas adsorption in

MOFs have employed standard, “generic,” Lennard-Jones-type force fields (e.g., UFF<sup>28</sup> or Drieding<sup>43</sup>) in combination with empirically fit adsorbate force fields (e.g., TraPPE<sup>30,44</sup> or EPM2).<sup>29</sup> Although there is some data benchmarking such force fields for screening purposes,<sup>45</sup> other works have shown substantial quantitative and sometimes even qualitative differences as compared to experiment, with particularly high discrepancies reported for ZIFs.<sup>46–49</sup> Furthermore, these standard force fields do not include explicit polarization, potentially leading to significant error when treating MOFs with strongly polar environments. As a benchmark, we compute gas uptake using our SAPT-FF force field to describe vdW interactions and explicitly incorporate CO<sub>2</sub> polarization.<sup>31</sup> With SAPT-FF, we have previously found semiquantitative to quantitative accuracy vs experimentally measured gas adsorption isotherms for a number of functionalized MOFs.<sup>20–23</sup> Since the force fields employ no empirical parameters, we anticipate similar accuracy for the present systems.

In Figure 3, we compare the predicted CO<sub>2</sub> uptake using the UFF/EPM2 force field to that computed using our SAPT-FF

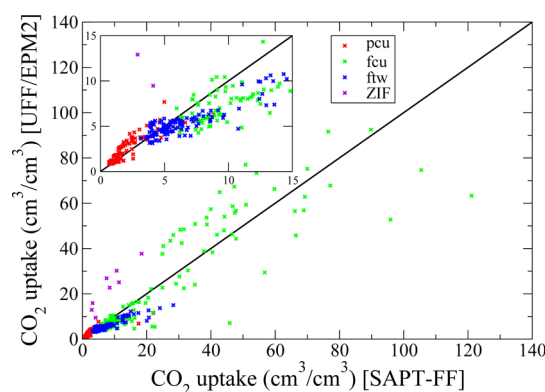


**Figure 3.** CO<sub>2</sub> uptake computed using UFF/EPM2 compared to that using SAPT-FF. Hypothetical MOFs are grouped according to their topology; pcu = red symbols, fcw = green symbols, and ftw = blue symbols. Experimental ZIF structures are shown as purple symbols (black line is  $y = x$  to guide the eye). For the total set,  $\text{SRCC}^2 = 0.90$ ,  $R^2 = 0.83$ , and slope = 0.91.

force field for the database of MOFs. There exists a relatively clear hierarchy among the MOF topologies, with  $\text{pcu} < \text{ftw} < \text{fcw}$  for low-pressure CO<sub>2</sub> uptake. This hierarchy seems to inversely correlate with the porosity of the MOFs within these topologies (*vide infra*), with low-porosity MOFs generally exhibiting higher CO<sub>2</sub> uptake. Significant quantitative differences in the prediction of CO<sub>2</sub> uptake between the two force fields exist, at least for a significant subset of the MOFs. In particular, UFF/EPM2 significantly overpredicts CO<sub>2</sub> uptake as compared to SAPT-FF for ZIFs, consistent with prior observations.<sup>21</sup> However, there are other MOFs, mainly of the ftw and fcw topology, for which SAPT-FF predicts higher uptake than UFF/EPM2. Despite these discrepancies and the dramatic differences in the underlying force fields, there is overall good correlation ( $\text{SRCC}^2 = 0.90$ ,  $R^2 = 0.83$ ) between the force field predictions, with UFF/EPM2 generally predicting slightly lower uptake (slope = 0.91). We partially attribute the high SRCC value to the 2 orders of magnitude variation in CO<sub>2</sub> uptake across the different topologies (pcu, fcw, ftw); the SRCC values computed for MOFs within each topology are significantly lower. Nonetheless, the strong

correlation suggests that generic force fields such as UFF may prove reliable for high-throughput screening predictions of low-pressure CO<sub>2</sub> uptake in MOFs (with no coordinatively unsaturated metal sites). However, the agreement between the predicted low-pressure gas uptakes at the UFF/EPM2 and SAPT-FF level obscures some crucial differences. As we will show below, this agreement is somewhat fortuitous, resulting from substantial cancellations in the differing treatments of short-range repulsion, long-range dispersion, and polarization between the force fields.

In Figure 4, we show a comparison of CO<sub>2</sub> uptakes computed with UFF/EPM2 compared to those computed

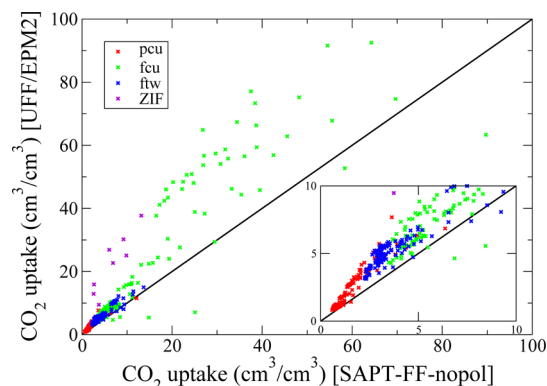


**Figure 4.** CO<sub>2</sub> uptake computed using UFF/EPM2 compared to that using SAPT-FF-nopol. Hypothetical MOFs are grouped according to their topology; pcu = red symbols, fcu = green symbols, and ftw = blue symbols. Experimental ZIF structures are shown as purple symbols (black line is  $y = x$  to guide the eye). For the total set, SRCC<sup>2</sup> = 0.94, R<sup>2</sup> = 0.86, and slope = 1.41.

with SAPT-FF *without* polarization (SAPT-FF-nopol) for the database of MOFs. This comparison isolates the differences in predicted uptake resulting from the different treatments of adsorbate–MOF vdW interactions. The slope of the best fit line (1.41) indicates that the UFF/EPM2 force field predicts systematically higher uptake than the SAPT-FF-nopol force field, resulting from the former’s generally stronger dispersion interaction energies between adsorbed CO<sub>2</sub> molecules and the MOF framework. This systematic trend has been previously noted<sup>21</sup> and is a consequence of the different functional forms for the dispersion interactions employed by the different force fields; the Lennard-Jones force field has a single  $C_6/R^6$  term to model vdW interactions, while the SAPT-FF functional form employs an extended  $C_n/R^n$  form ( $n = 6, 8, 10, 12$ ) to account for higher-order dispersion interactions. To accurately predict the binding of the minimum energy complex, the  $C_6$  term of the Lennard-Jones force field must be effectively ~30–40% larger to compensate for the neglect of higher order terms, yielding dispersion interactions which are asymptotically too attractive.<sup>50</sup> These small errors are magnified by the high density of atoms in the MOF crystal, resulting in systematic deviations in predictions of gas uptake.

We next seek to isolate the influence of adsorbate polarization. In Figure 5, we compare the CO<sub>2</sub> uptake as predicted by our SAPT-FF force field with (SAPT-FF) and without (SAPT-FF-nopol) polarization for the database of MOFs. As expected, we find that incorporation of adsorbate polarization yields substantially and systematically higher uptake (slope 0.65). However, while inclusion of polarization is essential for quantitatively accurate predictions, the high

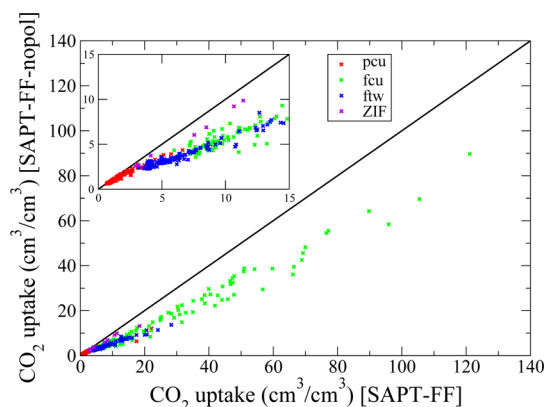


**Figure 5.** CO<sub>2</sub> uptake computed using SAPT-FF-nopol compared to that using SAPT-FF. Hypothetical MOFs are grouped according to their topology; pcu = red symbols, fcu = green symbols, and ftw = blue symbols. Experimental ZIF structures are shown as purple symbols (black line is  $y = x$  to guide the eye). For the total set, SRCC<sup>2</sup> = 0.98, R<sup>2</sup> = 0.98, and slope = 0.65.

degree of correlation (SRCC<sup>2</sup> = 0.98, R<sup>2</sup> = 0.98) between the force field predictions indicates that it may not be necessary in order to correctly rank (or prescreen) a similar database of MOFs. This is a significant result, as the inclusion of polarization in a force field requires substantially greater computational expense (typically, between 2 and 10 times).

Even when force fields predict similar gas uptakes, they may do so for different reasons (e.g., dissimilar distribution of adsorbates, differing “physics” of adsorption). We therefore compare the different force fields in more detail. Our lattice-model based approach for computing adsorption isotherms naturally yields a free-energy grid of each MOF, corresponding to a probability distribution of adsorbing a gas molecule at a discrete volume (~1 Å<sup>3</sup>) within the MOF. This probability distribution contains much more information than the resulting adsorption isotherm, yielding a far more informative analysis of the different treatments of physical interactions between gas molecules and the MOF.

To characterize the (dis)similarity of these probability distributions, we compute the Bhattacharyya coefficient (BC) of the distributions, defined as

$$BC(p, q) = \int \sqrt{p(r)q(r)} \, dr$$

where  $p(r)$  and  $q(r)$  are the respective probability distributions for adsorbing a CO<sub>2</sub> molecule within the MOF (with ~1 Å<sup>3</sup> resolution), as predicted by two different force fields. The BC coefficient is bounded by zero and one, with a value of one indicating perfect coincidence of the distributions.

Histograms of BC values derived from comparisons of different force fields are shown in Figure 6. The error cancellation resulting from the neglect of explicit polarization and overestimation of dispersion interactions, manifested in the computed CO<sub>2</sub> uptake for certain MOFs, does not appear in the adsorption site probability distributions. The absorption site probability distributions are less similar as predicted by the UFF/EPM2 and SAPT-FF force fields that employ different treatments of both polarization and vdW interactions (average BC = 0.86) than the distributions predicted by the force fields that only deviate in the treatment of one of these interactions (average BC = 0.92). This indicates that the error cancellation that leads to reasonable quantitative agreement in predicted

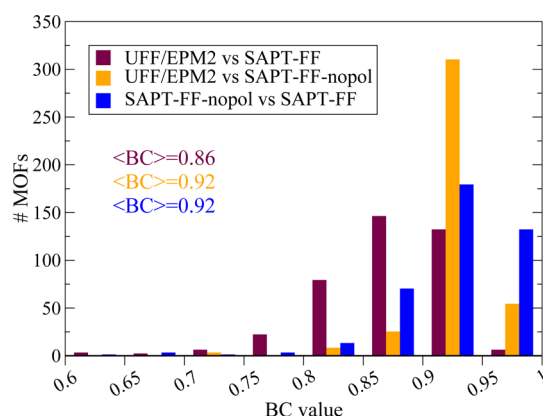


**Figure 6.** Histograms of BC values derived from comparisons of different force fields, showing the number of MOFs with the computed BC value. Distributions skewed toward one exhibit similar predicted distributions of adsorbates (within a given MOF) between the differing force fields.

CO<sub>2</sub> uptake by the UFF/EPM2 and SAPT-FF force fields is somewhat fortuitous. Thus, to the extent that these force fields differ primarily in their treatment of polarization and vdW interactions, the differing treatments of these physical interactions lead to different adsorption site distributions within each MOF.

We also illustrate the different effects of vdW and polarization interactions from another perspective. In Figure 7, we compare the energies of CO<sub>2</sub> molecules adsorbed in the minimum-energy adsorption sites for each MOF, as computed using different force fields. In Figure 7b, it is clear that the inclusion of explicit polarization systematically shifts the adsorption energy to more negative values at these sites, with greater shifts occurring for stronger binding, electrostatically dominated adsorption sites. In contrast to this, the comparison of minimum adsorption site energies as predicted using different vdW interactions (UFF/EPM2 vs SAPT-FF-nopol (Figure 7a)) shows no such obvious systematic shift.

Taken together, these comparisons suggest that generic, nonpolarizable force fields of the Lennard-Jones + Coulomb form may benefit from significant error cancellation resulting from both the neglect of explicit polarization and the overestimation of asymptotic dispersion interactions. While such error cancellation has been commonly exploited in liquid-state simulation (as evidenced by the great success of many nonpolarizable, Lennard-Jones + Coulomb force fields for neat

fluids), it is not *a priori* obvious that such error cancellation will be successful in MOFs due to their inhomogeneous and potentially highly polar nature. Thus, although our results suggest that generic force fields are likely sufficient for high-throughput prescreening of MOFs for gas adsorption, some caution is warranted.

**Enhancement of CO<sub>2</sub> Uptake by Incorporating Functional Groups in MOFs.** It is widely recognized that functionalization of organic SBUs with polar groups can enhance low-pressure CO<sub>2</sub> uptake in MOFs. We evaluated the performance of the seven functional groups present in our database of 424 MOFs, Cl, Br, NH<sub>2</sub>, OH, COOH, NO<sub>2</sub>, and COH (aldehyde), by computing the average percent enhancement in CO<sub>2</sub> uptake for the respective functionalized MOFs compared to their unfunctionalized “parent” structures. We note that each MOF is functionalized with only one type of group, either adding one (single) or two (double) functional groups to each organic SBU in the MOF. We find that, on average, the percent enhancement is generally linear with the number of functional groups (see Figure S13 in Supporting Information). Deviations from linearity can be seen for carboxylic acid groups, where double functionalization typically leads to more than twice the enhancement of single functionalization. This “synergistic” effect results from the simultaneous interaction of a gas molecule with two or more functional groups (usually on different SBUs), with nonlinear enhancements in uptake caused by the exponential form of the Boltzmann factor, as a consequence of the combination of adsorbate size, MOF pore size and topology, and linker functionalization.<sup>23</sup>

It is interesting to examine how the predicted enhancement depends on the choice of force field. In Figure 8, we show the percentage enhancement (for the case of double functionalization) of each organic SBU as predicted by three of the previously described adsorbate-MOF force fields: (1) SAPT-FF in combination with  $Q_{\text{SBU}}$  charges; (2) UFF/EPM2 in combination with  $Q_{\text{SBU}}$  charges; (3) UFF/EPM2 in combination with MEPO-QEq charges. From SAPT-FF/ $Q_{\text{SBU}}$ , we find that carboxylic acid functionalization enhances CO<sub>2</sub> uptake the most, followed by relatively similar average enhancements from NH<sub>2</sub>, OH, NO<sub>2</sub>, and COH, and typically lower enhancements from halogen functionalization. It is important to note that while amine functionalization can lead to very high CO<sub>2</sub> uptake enhancement through the formation of a carbamate species,<sup>51</sup> all amine functionalization in our database of MOFs is “aniline-like”, such that the NH<sub>2</sub> groups are adjacent to an aromatic

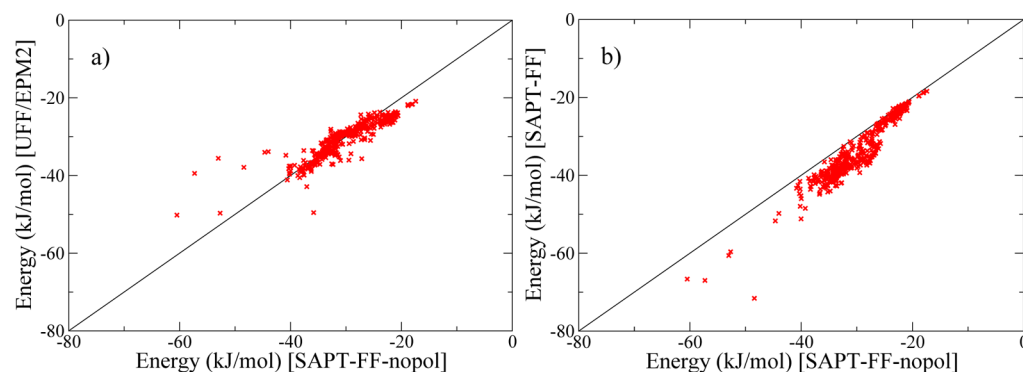


**Figure 7.** CO<sub>2</sub> minimum-energy adsorption site energies for each MOF, as predicted by different force fields: (a) comparison between UFF/EPM2 and SAPT-FF without polarization (SAPT-FF-nopol); (b) comparison between SAPT-FF with and without polarization.



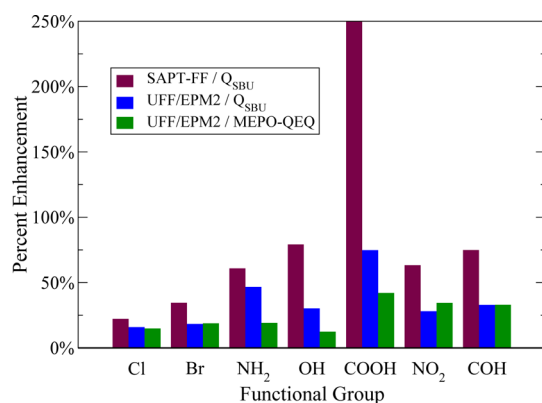


**Figure 8.** Average percent enhancement of CO<sub>2</sub> uptake at 298 K and 0.2 bar in MOFs with double functionalization per organic SBU relative to their unfunctionalized “parent” structures. Enhancements are predicted using three different force fields to describe adsorbate–MOF interactions: SAPT-FF in combination with  $Q_{SBU}$  charges (maroon), UFF/EPM2 in combination with  $Q_{SBU}$  charges (blue), and UFF/EPM2 in combination with MEPO-QEQ charges (green).

ring; such systems do not form carbamates and interact only via physisorption. This predicted qualitative ordering of enhancement is largely retained with the UFF/EPM2/ $Q_{SBU}$  force field combination; however, there exist *significant* quantitative differences in the predicted percentage enhancement in many cases, and in general UFF/EPM2/ $Q_{SBU}$  predicts lower functional group enhancement than SAPT-FF/ $Q_{SBU}$  (due in part to neglect of polarization as well as differences in predicted uptake of the parent structure). The third force field combination, UFF/EPM2/MEPO-QEQ, predicts a qualitatively different ordering compared to the other two force field combinations, implying that the prediction of functional group enhancement is relatively sensitive to electrostatics. These data are entirely consistent with the aggregate findings discussed above.

**Comparison of CH<sub>4</sub> Uptake in MOFs As Predicted by Different Force Fields.** Beyond CO<sub>2</sub> capture and separation, there is considerable interest in employing high-throughput screening to design MOFs optimized for high-pressure methane storage.<sup>2,8</sup> We have thus conducted a similar analysis to the above, computing methane uptake at 298 K, 30 bar and examined sensitivity to different force fields (qualitative conclusions at 100 bar are analogous but are omitted for brevity). Electrostatic interactions are generally negligible for methane and are omitted. The vdW interactions of a particular force field therefore completely determine the predicted methane uptake. We compare the prototypical UFF/TraPPE force field combination to SAPT-FF force field, comparing uptakes over our set of MOFs. All reported values are given in absolute uptake (volume of gas at STP adsorbed per volume of MOF).

The predicted methane uptake values at 298 K, 30 bar are compared in Figure 9. Note that while the CO<sub>2</sub> uptake at 0.2 bar spanned 2 orders of magnitude across the database of MOFs, the high-pressure CH<sub>4</sub> uptake values of the MOFs are within a factor of 4. One should thus expect lower correlation coefficients (at least SRCC) than for the CO<sub>2</sub> uptake. However, the correlation between force field predictions remains strong (SRCC<sup>2</sup> = 0.81,  $R^2$  = 0.90), and the slope of the best fit line is very close to one (1.04), indicating that UFF/TraPPE should be a solid choice for high-throughput screening of MOFs for

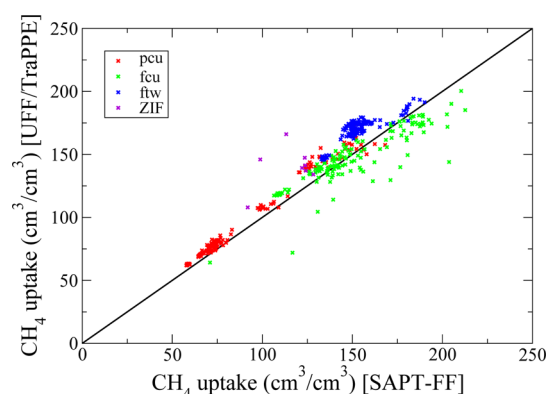


**Figure 9.** Methane uptake at 298 K, 30 bar predicted using UFF/TraPPE compared to that using the SAPT-FF force field. Hypothetical MOFs are grouped according to their topology; pcu = red symbols, fcu = green symbols, and ftw = blue symbols. Experimental ZIF structures are shown as purple symbols (black line is  $y = x$  to guide the eye). For the total set, SRCC<sup>2</sup> = 0.81,  $R^2$  = 0.90, and slope = 1.04.

high-pressure methane adsorption. The good agreement between force fields may not be surprising, as it has previously been shown that high-pressure methane uptake in MOFs is strongly correlated to the volumetric surface area and void fraction,<sup>2</sup> properties that are relatively insensitive to the details of the force field.

In order to gain deeper insight, we also examined the low-pressure portion of the 298 K isotherm at 1 bar (Figure 10). As

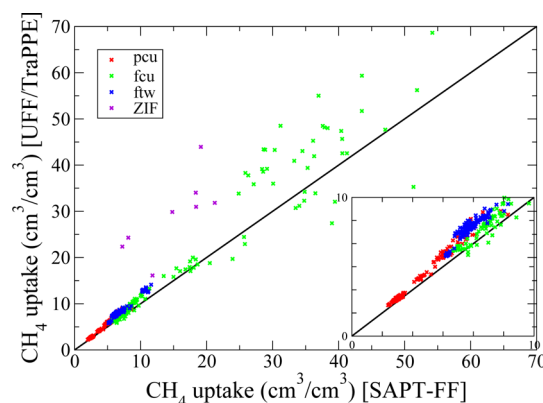


**Figure 10.** Methane uptake at 298 K, 1 bar predicted using UFF/TraPPE compared to that using the SAPT-FF force field. Hypothetical MOFs are grouped according to their topology; pcu = red symbols, fcu = green symbols, and ftw = blue symbols. Experimental ZIF structures are shown as purple symbols (black line is  $y = x$  to guide the eye). For the total set, SRCC<sup>2</sup> = 0.96,  $R^2$  = 0.92, and slope = 1.16.

evidenced by the slope of the best fit line (1.16), UFF/TraPPE generally predicts higher CH<sub>4</sub> uptake (at 1 bar) than SAPT-FF. This is analogous to our findings for CO<sub>2</sub> uptake, in which the treatment of adsorbate–MOF vdW interactions in the Lennard-Jones type force field led to a systematic prediction of higher gas uptake. On the basis of that analysis, we could anticipate that MOFs with smaller pores (and thus higher density of framework atoms) would exhibit larger deviations. In Figure 11, we compare the fractional deviation in uptake versus free volume fraction of the MOF (calculated as the He accessible free volume<sup>52</sup>), reflecting the expected trend. Similar to low-pressure CO<sub>2</sub> uptake, we find that low-pressure CH<sub>4</sub> uptake in ZIFs is highly sensitive to the choice of force field,



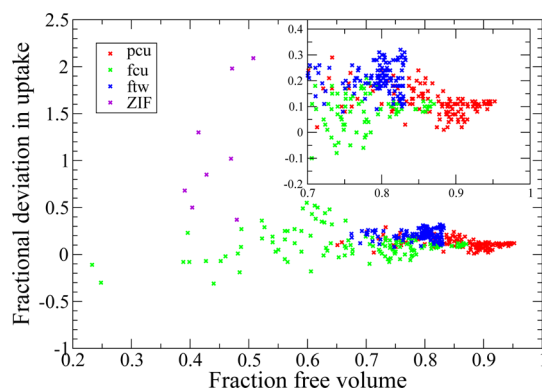


**Figure 11.** Fractional deviation of methane uptake at 298 K, 1 bar predicted using UFF/TraPPE and SAPT-FF force fields versus the free volume fraction of the MOF. Hypothetical MOFs are grouped according to their topology; pcu = red symbols, fcu = green symbols, and ftw = blue symbols. Experimental ZIF structures are shown as purple.

with UFF/TraPPE predicting 100–200% higher uptake than SAPT-FF for certain ZIFs. The observation that generic force fields significantly overpredict  $\text{CH}_4$  uptake in ZIFs has been previously demonstrated.<sup>46,48</sup> We attribute this to the fact that the ZIFs studied have relatively low free volume, with spherical or cylindrical pores, leading to many nonlocal interactions between adsorbed gas molecules and the atoms of the pore walls of the ZIF and compounding the overestimation of dispersion interactions.

## CONCLUDING REMARKS

Based upon merely a review of the recent literature, it is difficult to draw a uniform conclusion about the ability of generic force fields to accurately predict gas adsorption over a diverse set of MOFs: comparisons are often made for only a single MOF or sometimes involve “optimized” (i.e., adjusted to reproduce experimental results) force fields or utilize different vdW cutoffs, making it difficult to assess the reliability and robustness of standard force fields for high-throughput screening. In the present work, we circumvent this problem by comparing, for a diverse set of MOFs, against accurate “benchmark” *ab initio* force fields (SAPT-FF), which contain no empirical parameters and have been shown to semiquantitatively to quantitatively reproduce observed gas uptake on a diverse set of MOFs.

While gas uptake at high pressure seems to be relatively insensitive to the details of the force field (assuming accurate adsorbate–adsorbate potentials), screening low-pressure uptake places far more significant demands on the MOF–adsorbate potential. The relative accuracy of standard force fields depends on the type of adsorbate as well as the topology and functionalization of the MOF. For small, nonpolarizable adsorbates, adsorbed in very open, porous MOFs, standard force fields may predict uptake with good accuracy (our results give ~20% deviations for methane uptake in MOFs with >85% free volume). As the size of the adsorbate molecule increases, and the free volume of a MOF (porosity) decreases, the number of pairwise asymptotic dispersion interactions between adsorbate and MOF increases, and differences in the long-range tail of the vdW interactions of different force fields accumulate in the total adsorption energy. The effective  $C_6$  coefficients of Lennard-Jones force fields are generally 30–40% too large compared to the correct asymptotic dispersion interaction, causing the overprediction of methane uptake in MOFs of

lower free volume. For larger adsorbates such as  $\text{CO}_2$ , these quantitative deviations are magnified; however, this effect may be obscured by the neglect of explicit polarization. While polarization and vdW interactions have distinctly different effects on the adsorption site profile of a MOF, nonpolarizable Lennard-Jones force fields may benefit from error cancellation by neglecting the former interactions.

In spite of these quantitative differences, we generally find good correlation between the relative ranking of MOFs in terms of absolute gas uptake, as predicted by different force fields. For a high-throughput screening study, with the goal of identifying the top percentage of MOFs for a particular gas adsorption application, it may therefore be a reasonable approximation to employ generic force fields. But caution is still warranted. First, our set of hypothetical MOFs only encompasses three different topologies pcu, fcu, and ftw (in addition to the eight ZIFs, encompassing three additional topologies). In addition, the cancellation of errors from overestimation of dispersion and neglect of polarization is certainly not universal and, in fact, manifests itself in significant differences in the adsorbate probability density between standard and the *ab initio* force fields. These results suggest the very real possibility for significant breakdowns in at least particular classes of MOFs. We note that our study has focused on relatively nonpolar adsorbates ( $\text{CH}_4$  and  $\text{CO}_2$ ), and it is possible that some of the results/conclusions may not generalize to extremely polar adsorbates (e.g.,  $\text{H}_2\text{O}$ ).

Finally, it is interesting to note the general trend of high correlation coefficients between force field predictions, in spite of sometimes large and systematic quantitative deviations in predicted uptake (in particular for  $\text{CO}_2$ ). This may be best exemplified by the comparison of predicted  $\text{CO}_2$  uptake with and without charges (Figure 2); analogous trends were found by Kadantsev et al.<sup>35</sup> *A priori*, it is extremely surprising that such good correlation in predicted  $\text{CO}_2$  uptake between force fields exists even after completely eliminating electrostatic interactions, which constitute a major component of the MOF– $\text{CO}_2$  interaction. The explanation lies in the fact that the low-pressure  $\text{CO}_2$  adsorption of the set of hypothetical MOFs spans almost 2 orders of magnitude, with the gas uptake of particular MOFs largely predetermined by their topology and porosity, regardless of their particular functionalization. This has important implications for future high-throughput screening applications, as it should be possible to intelligently prescreen a large database of MOFs using descriptors based on detailed structural characteristics of the MOF, before any simulations are run; indeed, such a procedure has been successfully recently demonstrated.<sup>7,10</sup>

## ASSOCIATED CONTENT

### Supporting Information

Details of the construction, linkers, functional groups, and topologies of hypothetical MOFs; lattice-model simulation details; description of SAPT-based force field; all SAPT-FF force field parameters and combination rules utilized in this work; detailed description of  $Q_{\text{SBU}}$  charge fitting and implementation scheme; comparison of lattice-model and fully atomistic GCMC simulation predicted  $\text{CO}_2$  uptake; comparison of MEPO-QEq, no charges, and  $Q_{\text{SBU}}$  charges predictions of  $\text{CO}_2$  uptake employing SAPT-FF vdW interactions; 1 bar  $\text{CO}_2$  uptake results for all force field comparisons in this paper; single and double functional group enhancement of  $\text{CO}_2$  uptake; structures and  $Q_{\text{SBU}}$  charges of all

416 hypothetical MOFs. This material is available free of charge via the Internet at <http://pubs.acs.org>.

## AUTHOR INFORMATION

### Corresponding Author

\*E-mail: [schmidt@chem.wisc.edu](mailto:schmidt@chem.wisc.edu) (J.R.S.).

### Notes

R.Q.S. has a financial interest in the start-up company NuMat Technologies, which is seeking to commercialize metal-organic frameworks.

## ACKNOWLEDGMENTS

This work was partially supported by Chemical Sciences, Geosciences and Biosciences Division, Office of Basic Energy Sciences, Office of Science, U.S. Department of Energy, under Award DE-FG02-09ER16059 (J.G.M., J.R.S.). R.Q.S. gratefully acknowledges support from the Global Climate and Energy Project (GCEP). Computational resources were provided by the Center for High Throughput Computing at the University of Wisconsin.<sup>53</sup> The Northwestern authors also thank the National Energy Research Scientific Computing Center (NERSC), which is supported by the Office of Science of the U.S. Department of Energy under Contract DE-AC02-05CH11231, for computational resources. J.R.S. is an Alfred P. Sloan Research Fellow and a Camille Dreyfus Teacher-Scholar.

## REFERENCES

- (1) Watanabe, T.; Sholl, D. S. Accelerating Applications of Metal–Organic Frameworks for Gas Adsorption and Separation by Computational Screening of Materials. *Langmuir* **2012**, *28*, 14114–14128.
- (2) Wilmer, C. E.; Leaf, M.; Lee, C. Y.; Farha, O. K.; Hauser, B. G.; Hupp, J. T.; Snurr, R. Q. Large-Scale Screening of Hypothetical Metal–Organic Frameworks. *Nat. Chem.* **2012**, *4*, 83–89.
- (3) Colón, Y. J.; Fairen-Jimenez, D.; Wilmer, C. E.; Snurr, R. Q. High-Throughput Screening of Porous Crystalline Materials for Hydrogen Storage Capacity near Room Temperature. *J. Phys. Chem. C* **2014**, *118*, 5383–5389.
- (4) Wu, D.; Wang, C.; Liu, B.; Liu, D.; Yang, Q.; Zhong, C. Large-Scale Computational Screening of Metal–Organic Frameworks for CH<sub>4</sub>/H<sub>2</sub> Separation. *AIChE J.* **2012**, *58*, 2078–2084.
- (5) Haldoupis, E.; Nair, S.; Sholl, D. S. Efficient Calculation of Diffusion Limitations in Metal Organic Framework Materials: A Tool for Identifying Materials for Kinetic Separations. *J. Am. Chem. Soc.* **2010**, *132*, 7528–7539.
- (6) Wilmer, C. E.; Farha, O. K.; Bae, Y.-S.; Hupp, J. T.; Snurr, R. Q. Structure–Property Relationships of Porous Materials for Carbon Dioxide Separation and Capture. *Energy Environ. Sci.* **2012**, *5*, 9849–9856.
- (7) Fernandez, M.; Trefiak, N. R.; Woo, T. K. Atomic Property Weighted Radial Distribution Functions Descriptors of Metal–Organic Frameworks for the Prediction of Gas Uptake Capacity. *J. Phys. Chem. C* **2013**, *117*, 14095–14105.
- (8) Fernandez, M.; Woo, T. K.; Wilmer, C. E.; Snurr, R. Q. Large-Scale Quantitative Structure–Property Relationship (QSPR) Analysis of Methane Storage in Metal–Organic Frameworks. *J. Phys. Chem. C* **2013**, *117*, 7681–7689.
- (9) Wu, D.; Yang, Q.; Zhong, C.; Liu, D.; Huang, H.; Zhang, W.; Maurin, G. Revealing the Structure–Property Relationships of Metal–Organic Frameworks for CO<sub>2</sub> Capture from Flue Gas. *Langmuir* **2012**, *28*, 12094–12099.
- (10) Fernandez, M.; Boyd, P. G.; Daff, T. D.; Aghaji, M. Z.; Woo, T. K. Rapid and Accurate Machine Learning Recognition of High Performing Metal Organic Frameworks for CO<sub>2</sub> Capture. *J. Phys. Chem. Lett.* **2014**, *5*, 3056–3060.
- (11) Kim, J.; Abouelnasr, M.; Lin, L.-C.; Smit, B. Large-Scale Screening of Zeolite Structures for CO<sub>2</sub> Membrane Separations. *J. Am. Chem. Soc.* **2013**, *135*, 7545–7552.
- (12) Kim, J.; Lin, L.-C.; Martin, R. L.; Swisher, J. A.; Haranczyk, M.; Smit, B. Large-Scale Computational Screening of Zeolites for Ethane/Ethene Separation. *Langmuir* **2012**, *28*, 11914–11919.
- (13) Kim, J.; Lin, L.-C.; Swisher, J. A.; Haranczyk, M.; Smit, B. Predicting Large CO<sub>2</sub> Adsorption in Aluminosilicate Zeolites for Postcombustion Carbon Dioxide Capture. *J. Am. Chem. Soc.* **2012**, *134*, 18940–18943.
- (14) Haldoupis, E.; Nair, S.; Sholl, D. S. Pore Size Analysis of >250 000 Hypothetical Zeolites. *Phys. Chem. Chem. Phys.* **2011**, *13*, 5053–5060.
- (15) Earl, D. J.; Deem, M. W. Toward a Database of Hypothetical Zeolite Structures. *Ind. Eng. Chem. Res.* **2006**, *45*, 5449–5454.
- (16) Colon, Y. J.; Snurr, R. Q. High-Throughput Computational Screening of Metal–Organic Frameworks. *Chem. Soc. Rev.* **2014**, *43*, 5735–5749.
- (17) Kim, J.; Smit, B. Efficient Monte Carlo Simulations of Gas Molecules Inside Porous Materials. *J. Chem. Theory Comput.* **2012**, *8*, 2336–2343.
- (18) Yu, K.; McDaniel, J. G.; Schmidt, J. R. An Efficient Multi-Scale Lattice Model Approach to Screening Nano-Porous Adsorbents. *J. Chem. Phys.* **2012**, *137*, 244102.
- (19) Jeziorski, B.; Moszynski, R.; Szalewicz, K. Perturbation-Theory Approach to Intermolecular Potential-Energy Surfaces of Van-Der-Waals Complexes. *Chem. Rev.* **1994**, *94*, 1887–1930.
- (20) McDaniel, J. G.; Yu, K.; Schmidt, J. R. Ab Initio, Physically Motivated Force Fields for CO<sub>2</sub> Adsorption in Zeolitic Imidazolate Frameworks. *J. Phys. Chem. C* **2011**, *116*, 1892–1903.
- (21) McDaniel, J. G.; Schmidt, J. R. Robust, Transferable, and Physically-Motivated Force Fields for Gas Adsorption in Functionalized Zeolitic Imidazolate Frameworks. *J. Phys. Chem. C* **2012**, *116*, 14031–14039.
- (22) McDaniel, J. G.; Schmidt, J. R. Physically-Motivated Force Fields from Symmetry-Adapted Perturbation Theory. *J. Phys. Chem. A* **2013**, *117*, 2053–2066.
- (23) McDaniel, J. G.; Yu, K.; Schmidt, J. R. Microscopic Origins of Enhanced Gas Adsorption and Selectivity in Mixed-Linker Metal–Organic Frameworks. *J. Phys. Chem. C* **2013**, *117*, 17131–17142.
- (24) Bae, Y.-S.; Liu, J.; Wilmer, C. E.; Sun, H.; Dickey, A. N.; Kim, M. B.; Benin, A. I.; Willis, R. R.; Barpaga, D.; LeVan, M. D.; Snurr, R. Q. The Effect of Pyridine Modification of Ni-DOBDC on CO<sub>2</sub> Capture under Humid Conditions. *Chem. Commun.* **2014**, *50*, 3296–3298.
- (25) Dzubak, A. L.; Lin, L.-C.; Kim, J.; Swisher, J. A.; Poloni, R.; Maximoff, S. N.; Smit, B.; Gagliardi, L. Ab Initio Carbon Capture in Open-Site Metal–Organic Frameworks. *Nat. Chem.* **2012**, *4*, 810–816.
- (26) Chen, L. J.; Grajciar, L.; Nachtigall, P.; Duren, T. Accurate Prediction of Methane Adsorption in a Metal–Organic Framework with Unsaturated Metal Sites by Direct Implementation of an ab Initio Derived Potential Energy Surface in GCMC Simulation. *J. Phys. Chem. C* **2011**, *115*, 23074–23080.
- (27) Essmann, U.; Perera, L.; Berkowitz, M. L.; Darden, T.; Lee, H.; Pedersen, L. G. A Smooth Particle Mesh Ewald Method. *J. Chem. Phys.* **1995**, *103*, 8577–8593.
- (28) Rappe, A. K.; Casewit, C. J.; Colwell, K. S.; Goddard, W. A.; Skiff, W. M. UFF, A Full Periodic-Table Force-Field for Molecular Mechanics and Molecular-Dynamics Simulations. *J. Am. Chem. Soc.* **1992**, *114*, 10024–10035.
- (29) Harris, J. G.; Yung, K. H. Carbon Dioxides Liquid-Vapor Coexistence Curve and Critical Properties as Predicted by a Simple Molecular-Model. *J. Phys. Chem.* **1995**, *99*, 12021–12024.
- (30) Martin, M. G.; Siepmann, J. I. Transferable Potentials for Phase Equilibria. I. United-Atom Description of n-Alkanes. *J. Phys. Chem. B* **1998**, *102*, 2569–2577.
- (31) Yu, K.; McDaniel, J. G.; Schmidt, J. R. Physically Motivated, Robust, ab Initio Force Fields for CO<sub>2</sub> and N<sub>2</sub>. *J. Phys. Chem. B* **2011**, *115*, 10054–10063.

- (32) Liu, H.; Silva, C. M.; Macedo, E. A. New Equations for Tracer Diffusion Coefficients of Solutes in Supercritical and Liquid Solvents Based on the Lennard-Jones Fluid Model. *Ind. Eng. Chem. Res.* **1997**, *36*, 246–252.
- (33) Wilmer, C. E.; Kim, K. C.; Snurr, R. Q. An Extended Charge Equilibration Method. *J. Phys. Chem. Lett.* **2012**, *3*, 2506–2511.
- (34) Haldoupis, E.; Nair, S.; Sholl, D. S. Finding MOFs for Highly Selective CO<sub>2</sub>/N<sub>2</sub> Adsorption Using Materials Screening Based on Efficient Assignment of Atomic Point Charges. *J. Am. Chem. Soc.* **2012**, *134*, 4313–4323.
- (35) Kadantsev, E. S.; Boyd, P. G.; Daff, T. D.; Woo, T. K. Fast and Accurate Electrostatics in Metal Organic Frameworks with a Robust Charge Equilibration Parameterization for High-Throughput Virtual Screening of Gas Adsorption. *J. Phys. Chem. Lett.* **2013**, *4*, 3056–3061.
- (36) Stone, A. J. Distributed Multipole Analysis, or How to Describe a Molecular Charge-Distribution. *Chem. Phys. Lett.* **1981**, *83*, 233–239.
- (37) Stone, A. J.; Alderton, M. Distributed Multipole Analysis - Methods and Applications. *Mol. Phys.* **1985**, *56*, 1047–1064.
- (38) Ferenczy, G. G. Charges Derived from Distributed Multipole Series. *J. Comput. Chem.* **1991**, *12*, 913–917.
- (39) Campañá, C.; Mussard, B.; Woo, T. K. Electrostatic Potential Derived Atomic Charges for Periodic Systems Using a Modified Error Functional. *J. Chem. Theory Comput.* **2009**, *5*, 2866–2878.
- (40) Chen, D.-L.; Stern, A. C.; Space, B.; Johnson, J. K. Atomic Charges Derived from Electrostatic Potentials for Molecular and Periodic Systems. *J. Phys. Chem. A* **2010**, *114*, 10225–10233.
- (41) Watanabe, T.; Manz, T. A.; Sholl, D. S. Accurate Treatment of Electrostatics during Molecular Adsorption in Nanoporous Crystals without Assigning Point Charges to Framework Atoms. *J. Phys. Chem. C* **2011**, *115*, 4824–4836.
- (42) Rappe, A. K.; Goddard, W. A. Charge Equilibration for Molecular Dynamics Simulations. *J. Phys. Chem.* **1991**, *95*, 3358–3363.
- (43) Mayo, S. L.; Olafson, B. D.; Goddard, W. A. Dreiding - A Generic Force-Field for Molecular Simulations. *J. Phys. Chem.* **1990**, *94*, 8897–8909.
- (44) Potoff, J. J.; Siepmann, J. I. Vapor-Liquid Equilibria of Mixtures Containing Alkanes, Carbon Dioxide, and Nitrogen. *AIChE J.* **2001**, *47*, 1676–1682.
- (45) Yazaydin, A. O.; Snurr, R. Q.; Park, T.-H.; Koh, K.; Liu, J.; LeVan, M. D.; Benin, A. I.; Jakubczak, P.; Lanuza, M.; Galloway, D. B.; Low, J. J.; Willis, R. R. Screening of Metal–Organic Frameworks for Carbon Dioxide Capture from Flue Gas Using a Combined Experimental and Modeling Approach. *J. Am. Chem. Soc.* **2009**, *131*, 18198–18199.
- (46) Liu, B.; Smit, B. Molecular Simulation Studies of Separation of CO<sub>2</sub>/N<sub>2</sub>, CO<sub>2</sub>/CH<sub>4</sub>, and CH<sub>4</sub>/N<sub>2</sub> by ZIFs. *J. Phys. Chem. C* **2010**, *114*, 8515–8522.
- (47) Rankin, R. B.; Liu, J. C.; Kulkarni, A. D.; Johnson, J. K. Adsorption and Diffusion of Light Gases in ZIF-68 and ZIF-70: A Simulation Study. *J. Phys. Chem. C* **2009**, *113*, 16906–16914.
- (48) Perez-Pellitero, J.; Amrouche, H.; Siperstein, F. R.; Pirngruber, G.; Nieto-Draghi, C.; Chaplais, G.; Simon-Masseron, A.; Bazer-Bachi, D.; Peralta, D.; Bats, N. Adsorption of CO<sub>2</sub>, CH<sub>4</sub>, and N<sub>2</sub> on Zeolitic Imidazolate Frameworks: Experiments and Simulations. *Chem.—Eur. J.* **2010**, *16*, 1560–1571.
- (49) Battisti, A.; Taioli, S.; Garberoglio, G. Zeolitic Imidazolate Frameworks for Separation of Binary Mixtures of CO<sub>2</sub>, CH<sub>4</sub>, N<sub>2</sub> and H<sub>2</sub>: A Computer Simulation Investigation. *Microporous Mesoporous Mater.* **2011**, *143*, 46–53.
- (50) Misquitta, A. J.; Stone, A. J. Dispersion Energies for Small Organic Molecules: First Row Atoms. *Mol. Phys.* **2008**, *106*, 1631–1643.
- (51) Demessence, A.; D'Alessandro, D. M.; Foo, M. L.; Long, J. R. Strong CO<sub>2</sub> Binding in a Water-Stable, Triazolate-Bridged Metal–Organic Framework Functionalized with Ethylenediamine. *J. Am. Chem. Soc.* **2009**, *131*, 8784–8786.
- (52) Babarao, R.; Hu, Z. Q.; Jiang, J. W.; Chempath, S.; Sandler, S. I. Storage and Separation of CO<sub>2</sub> and CH<sub>4</sub> in Silicalite, C-168 Schwarzite, and IRMOF-1: A Comparative Study from Monte Carlo Simulation. *Langmuir* **2007**, *23*, 659–666.
- (53) Litzkow, M.; Livney, M.; Mutka, M. *Condor - A Hunter of Idle Workstations*; IEEE: New York, 1988.